Instabilities in the flow around an impulsively rotated sphere

Sophie A. W. Calabretto* and James P. Denier†
Department of Mathematics and Statistics, Macquarie University, Sydney 2091, Australia

(Received 20 March 2019; published 16 July 2019)

When a sphere, suspended in an otherwise quiescent fluid, is rotated, the resulting flow exhibits a wide range of fundamental fluid physics, ranging from the collision of boundary layers through to the development of radial jets and subsequent absolute instabilities in the spatially and temporally developing flow. In this way, such a flow provides a paradigm for the study of instabilities in temporally and spatially developing boundary layers. There is a body of experimental work on this problem Y. Kohama and R. Kobayashi, J. Fluid Mech. **137**, 153 (1983); T. Hada and A. Ito, Trans. Vis. Soc. Jpn. **23**, 231 (2003) that suggests that the flow within the sphere's boundary layer can be unstable to spiral vortices for moderate rotation rates; however, other experiments F. P. Bowden and R. G. Lord, Proc. R. Soc. London A **271**, 143 (1963); F. Kreith *et al.*, Int. J. Heat Mass Transfer **6**, 881 (1963); S. A. W. Calabretto *et al.* (unpublished) demonstrate that the flow over the sphere remains laminar until much higher rotation rates. We consider this problem from a computational perspective, seeking to understand how, when, and where such instabilities may develop. Our results show good agreement with the experiments of Kreith *et al.* and Calabretto *et al.* in that the flow over much of the boundary layer remains undisturbed and, additionally, the spiral vortex instabilities that develop in the flow are convective in nature.

DOI: 10.1103/PhysRevFluids.4.073904

I. INTRODUCTION

The flow induced by rotating solid bodies is one of considerable importance in fluid mechanics. Within this broad class of flows, the flow exterior to a rotating sphere provides a paradigm for the study of many fundamental questions in fluid mechanics, in particular the phenomena of boundary-layer collisions and unsteady boundary-layer separation. If a sphere, immersed in a body of fluid and initially at rest, is imparted with angular momentum, the boundary layer that develops on the sphere's surface is advected around the sphere from the poles to collide at the equator. The study of this boundary-layer development process and subsequent collision has a long history, first being considered by Howarth [1] and subsequently by Banks [2,3] as well as Banks and Zaturska [4]. The latter study demonstrated that the boundary-layer collision manifests in the boundary-layer equations through the development of a finite-time singularity. The structure of this singularity, and the time at which it occurs, was first considered by Simpson and Stewartson [5], later by Dennis and Duck [6], and subsequently by van Dommelen [7]. Using the Lagrangian approach developed by Cowley *et al.* [8], van Dommelen was able to obtain a more accurate prediction of the time for the onset of the finite-time singularity.

The early 1960s saw the publication of two papers describing experiments on the flow induced by a rotating sphere. The first, conducted by Bowden and colleagues [9,10], employed a metal sphere that was magnetically levitated and spun using induction. Inductive heating of the surface of the

*sophie.calabretto@mq.edu.au
†jim.denier@mq.edu.au

sphere served to change the density of the fluid within the boundary layer on the sphere, allowing for flow visualization using Schlieren photography. Such flow visualization allowed Bowden and Lord [9] to observe the radial jet that is ejected from the sphere's surface at the equator, and is a direct result of the collision of the boundary layers induced upon spin up of the sphere.

Interestingly, Bowden and Lord [9] comment that the flow in their work may be assumed to be laminar, seemingly basing this assertion on the fact that at the time their experiments were conducted, the critical value of the Reynolds number for transition to turbulence on a rotating disk was approximately 3×10^5 and the maximum value of their Reynolds numbers was considerably lower than this (the maximum Reynolds in their experiments, shown in Fig. 1 of [9], was approximately 7700). They make no further comment about the flow within the boundary layer and make no mention of observing instabilities in this region. They do, however, comment on the radial jet and make note that as the Reynolds number increases, it becomes shortened due to it becoming turbulent.

The second set of experiments, undertaken around the same time as [9], was performed by Kreith *et al.* [11]. These experiments were conducted in a similar manner to [9], using small metal spheres, which were heated and thus allowing measurements on natural and forced convection to be undertaken. In addition to these metal spheres, they also employed (much larger) *ebonite* bowling balls. At the time of their experiments, there were no set tolerances on the manufacture of such balls, although they were generally considered "smooth." We note that recent requirements have provided clear tolerances on such bowling balls, which can have surface roughness no larger than 1.27 μm. In the context of the overall dimensions of a bowling ball (of diameter 21.83 cm), this equates to a potential roughness of less than approximately 0.0006% of the ball's diameter.

The experimental images provided by Kreith *et al.* [11] show no real evidence of instabilities within the boundary layer for flow Reynolds numbers up to $\mathrm{Re}_d = 34\,000$ (the Reynolds number defined with respect to the sphere's diameter), but do show evidence of an instability in the form of spiral vortices at a higher Reynolds number of $\mathrm{Re}_d = 54\,000$. At their highest Reynolds numbers, Ref. [11] presents no evidence of a boundary-layer instability; see their Fig. 10. Interestingly, Kreith *et al.* [11] note that they observed flow that was "laminar over most of the sphere even when the rotational speed was increased, but increasing the Reynolds number broadened the separation zone at the equator" p. 890. They conclude by noting that at "Reynolds numbers below $\mathrm{Re}_d = 5\times10^5$ the flow induced by a sphere rotating in an infinite environment is laminar except for a small region in the vicinity of the equator where the boundary layers from the two halves of the sphere meet" p. 890.

We note at this point that we will make reference to a Reynolds number based upon the sphere's radius a and the final angular velocity of the sphere Ω, defined according to

$$\mathrm{Re} = \frac{\Omega a^2}{\nu}.$$

In the earlier experiments of Kreith *et al.* [11], they defined a Reynolds number as $\mathrm{Re}_d = \Omega d_s^2/\nu_f$, where ν_f is the kinematic viscosity of the fluid (in their case, air), d_s is the diameter of the sphere, and Ω the final rotation rate of the sphere. In discussing their results, we therefore note a factor of four difference; their Reynolds number Re_d is four times our Reynolds number.

In the years following the experiments of Bowden and Lord [9] and Kreith *et al.* [11], there have been a number of other experimental studies on the transition to turbulence on the surface (that is, within the boundary layer) of a rotating sphere. Most important among these are those conducted by Kohama and Kobayashi [12] who show that an instability can develop within the boundary layer at a latitude of roughly 70 degrees from the equator at Reynolds numbers above approximately $\mathrm{Re} = 11\,000$.

Even more recent experiments by Hada and Ito [13] explore the breakdown of the radial jet, showing images that suggest an absolute instability, developing for flow Reynolds numbers as low as $\mathrm{Re} = 2600$. This absolute instability in the jet has been confirmed by the computational results of Calabretto *et al.* [14,15], and also seen in the more recent experiments of Calabretto *et al.* [16]; in

the latter, the instability was identified as being due to a precession in the sphere, itself the result of small, measurable imperfections in the manufacture of their sphere experiment. Hada and Ito [13] also observe spiral vortices, but do not report a critical Reynolds number at which they first appear, whereas Calabretto and co-workers [14,16] found no evidence of these spiral vortices.

Like the sphere employed by [11], the recent experiments of Calabretto *et al.* [16] also used spheres that were "very smooth," employing pool balls that were manufactured to a very high tolerance with a measured "local roughness" of around 1 μm (compared to the ball radius of 28 560 μm [see 17]), an order of magnitude larger than any roughness in [11]. This roughness of 0.004% nevertheless fits the description of "very smooth." In contrast, the experiments of [12] and [13] employed metal spheres that although polished, were also painted (black) to facilitate flow visualization. This additional coating presents the opportunity to introduce roughness onto the sphere's surface that may, through a roughness-induced receptivity, serve to introduce a small, but finite disturbance to the flow.

Various attempts to predict the critical Reynolds number for the formation of instabilities within the sphere's boundary layer have appeared over the past decade. The work of Garrett and Peake [18], which employed a combined local, steady, and parallel flow assumption on the basic flow, did demonstrate that the flow was susceptible to an instability that manifests physically as a spiral vortex. More recent work by Barrow *et al.* [19] considered the problem from the context of a global stability analysis, predicting a self-excited linear global mode at latitudes between 55° and 65°. Recently, Segalini and Garrett [20] employed a steady solution of the full flow equations, which was patched together from the asymptotic descriptions of the boundary layer, the jet, and the boundary-layer-jet junction region at the equator, to explore the nonparallel stability of the flow. This analysis made use of the structure proposed by Smith and Duck [21] to describe the region at the equator where colliding boundary layers erupt to produce the radial jet. Calabretto *et al.* [16] presented both experimental and computational results that demonstrate that this structure is incorrect. This calls into question the validity of the analysis presented in [20].

We therefore have two groups of experiments, one of which predicts instability for relatively low Reynolds number, $\mathrm{Re} \approx 11\,000$, while the other shows the boundary layer to remain largely stable over most of its extent at much higher Reynolds numbers. Our aim here is to explore this problem from a computational standpoint; we will present results that indicate that the spiral vortices can develop within the boundary layer, but that these are convective instabilities which are convected out of the boundary layer and into the radial jet, leaving the boundary-layer flow over most of the sphere undisturbed and laminar.

II. FORMULATION

As our concern here is with the development of instabilities within the boundary layer, well away from the equatorial plain, we choose to apply equatorial symmetry to the computational domain. Such a formulation has two advantages. Firstly, it naturally suppresses the absolute instability that develops in the radial jet at the equator (see [14]). Calabretto *et al.* [14] demonstrated that this absolute instability in the jet propagates back towards the sphere but does not, at least for the Reynolds numbers they considered, impact upon the boundary-layer flow on the sphere's surface. Thus, by imposing a symmetry condition, we are able to limit the computational expense that would be required in resolving the motion in the radial jet. The second reason is a simple consequence of the symmetry condition, allowing us to focus our computational efforts on only half of the computational domain. It is important to note that the imposition of this symmetry condition does not impact the flow evolution within the sphere's boundary layer. We present results to this effect at the end of Sec. III.

From a computational perspective, it proves challenging to impose an instantaneous change in the rotation rate of the sphere. We therefore choose to ramp up the rotation rate from zero to a constant value in a linear fashion, over a small, but finite time t_s. We therefore set our angular velocity on the sphere's surface, $r = 1$, to be $\tilde{\Omega}(t)$. When referenced in terms of spherical polar coordinates

(r, θ, ϕ), where $\theta = 0$ is the equator and $\theta = \pi$ is the pole, with corresponding velocity components (u_r, u_θ, u_ϕ), the Navier-Stokes equations must be solved subject to the boundary conditions

$$u_r = u_\theta = 0, \quad u_\phi = \tilde{\Omega}(t)\cos\theta \quad \text{on} \quad r = 1.$$

The function $\tilde{\Omega}(t)$ is given by

$$\tilde{\Omega}(t) = \begin{cases} 0 & \text{for} \quad t < 0, \\ \dfrac{2t}{\sqrt{(t_s - t)^2} + t_s + t} & \text{for} \quad t \geqslant 0, \end{cases}$$

where $t_s > 0$ is defined as the ramp-up time (that is, the time taken for the sphere to be spun up to its final angular velocity). All results reported here are for a time $t_s = 0.05$. The effect of changing t_s is minimal and does not impact any of the results presented here; details of the effect of these changes can be found in Ref. [22].

In addition to the boundary condition at the sphere's surface, the flow must also satisfy the full no-slip boundary conditions on the boundaries of the container in which the sphere resides.

Without any external disturbances, the flow would not develop any spiral instability. We must therefore induce this instability by introducing an appropriate disturbance into the flow. Two possible options are available, each presenting a different physical receptivity mechanism. The first approach would correspond physically to a small surface imperfection. Such a surface imperfection is know to induce centrifugal instabilities in boundary layers [23], the instability problem then being posed as one of flow *receptivity*. In practice, if we take the sphere surface to be

$$r = 1 + \epsilon\Delta(\theta, \phi),$$

where $0 < \epsilon \ll 1$, we can then make a simple change of coordinates in the Navier-Stokes equations via

$$\hat{r} = r - \epsilon\Delta(\theta, \phi).$$

This approach serves well when considering a receptivity mechanism induced by surface roughness. However, as noted earlier, the experiments of [14,16] and the earlier experiments by [11] were conducted using spheres that were very smooth (in both cases, polished spheres, manufactured to high tolerances for low surface roughness). Surface roughness was not a concern in the experiments of [9], who were primarily interested in fundamental questions regarding abrasion. The later experiments by [12] and [13] employed metal spheres that were painted black (after polishing). The recent experiments by Calabretto *el al*. [16], and those of [11], can therefore be seen as limiting surface-roughness effects, whereas the experiments of [12] and [13] may, despite all attempts to mitigate roughness, have introduced some element of roughness to their experiments. To explore theoretically the delayed transition found in [14,16] and [11], we will model a smooth sphere and introduce a disturbance through another mechanism, aiming to model an "external" disturbance to the sphere's boundary layer.

We solve this problem numerically using SEMTEX, a quadrilateral spectral element direct numerical solver, which uses parametrically mapped elements and, hence, whose capabilities are readily adapted to the spherical geometry considered here. For the problem to be computationally tractable, we first embed the sphere within a larger volume of fluid contained in a large, finite container. This allows us to apply full physical no-slip boundary conditions on all rigid surfaces (that is, the sphere's surface and the bounding container). The computational container's dimensions were suitably large so as to ensure that the outer rigid boundaries did not affect the flow dynamics, at least for the timescales considered here. To appropriately capture the behavior of the boundary layer, we employ a fine mesh of elements around the circumference of the sphere, each element containing a computational mesh of 10×10 Lagrange knot points. This ensures that our computations are fully resolved and accurately capture the dynamics of the thin boundary layer and the jet region; extensive tests were undertaken in this regard to ensure that all results presented here are well resolved.

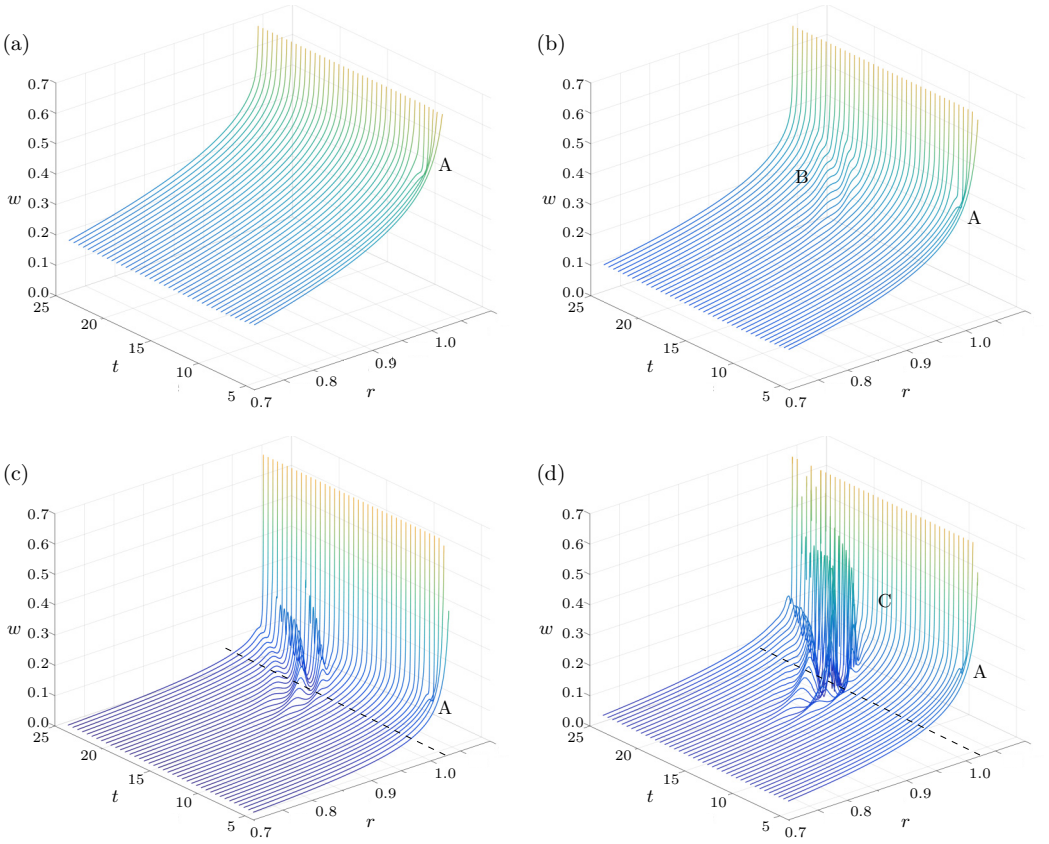

FIG. 1. The temporal evolution of the azimuthal velocity at 0.02 radii from the sphere's surface for a flow Reynolds numbers (a) $\mathrm{Re} = 8\times10^3$, (b) $\mathrm{Re} = 1\times10^4$, (c) $\mathrm{Re} = 2.4\times10^4$, and (d) $\mathrm{Re} = 3\times10^4$. In all cases, the flow disturbance was introduced at a latitudinal location of $\theta = 70^\circ$.

Additionally, extensive tests were undertaken to ensure that the flow induced by the rotating sphere was not affected by any interaction with the walls of the larger container on the timescales we consider; we use a total of 2916 elements in the cross plane to ensure no interaction, with 80 azimuthal modes (over $\phi = \pi$) in order to capture any smaller-scale dynamics propagating in the azimuthal direction. In all our calculations, the temporal time stepping is accomplished via a second-order backwards-differencing scheme (see [24]); the time step Δt was set to 2×10^{-4}, and convergence tests demonstrated that this was more than sufficient for our computations. A typical run, parallelized across 40 processors (hyperthreaded to allow for multiple runs at once), would generally see computational wall times of approximately two and a half weeks to compute 20 seconds of "real time" solution.

In order to impose a disturbance to the flow, the flow is evolved from an initial state of rest, to a time $t = 4$. At this point, a disturbance is added to the velocity field at a particular latitudinal location, measured from the equator, and at a fixed distance from the sphere (within the boundary layer). This disturbance aims to mimic an impulsive, Dirac-δ functionlike forcing to the flow, similar to that employed in classical studies of absolute instabilities in boundary layers.

III. RESULTS

The fact that the flow develops both temporally and spatially provides some challenges in presenting the results of our study. For this reason, we choose to first present results in the form of

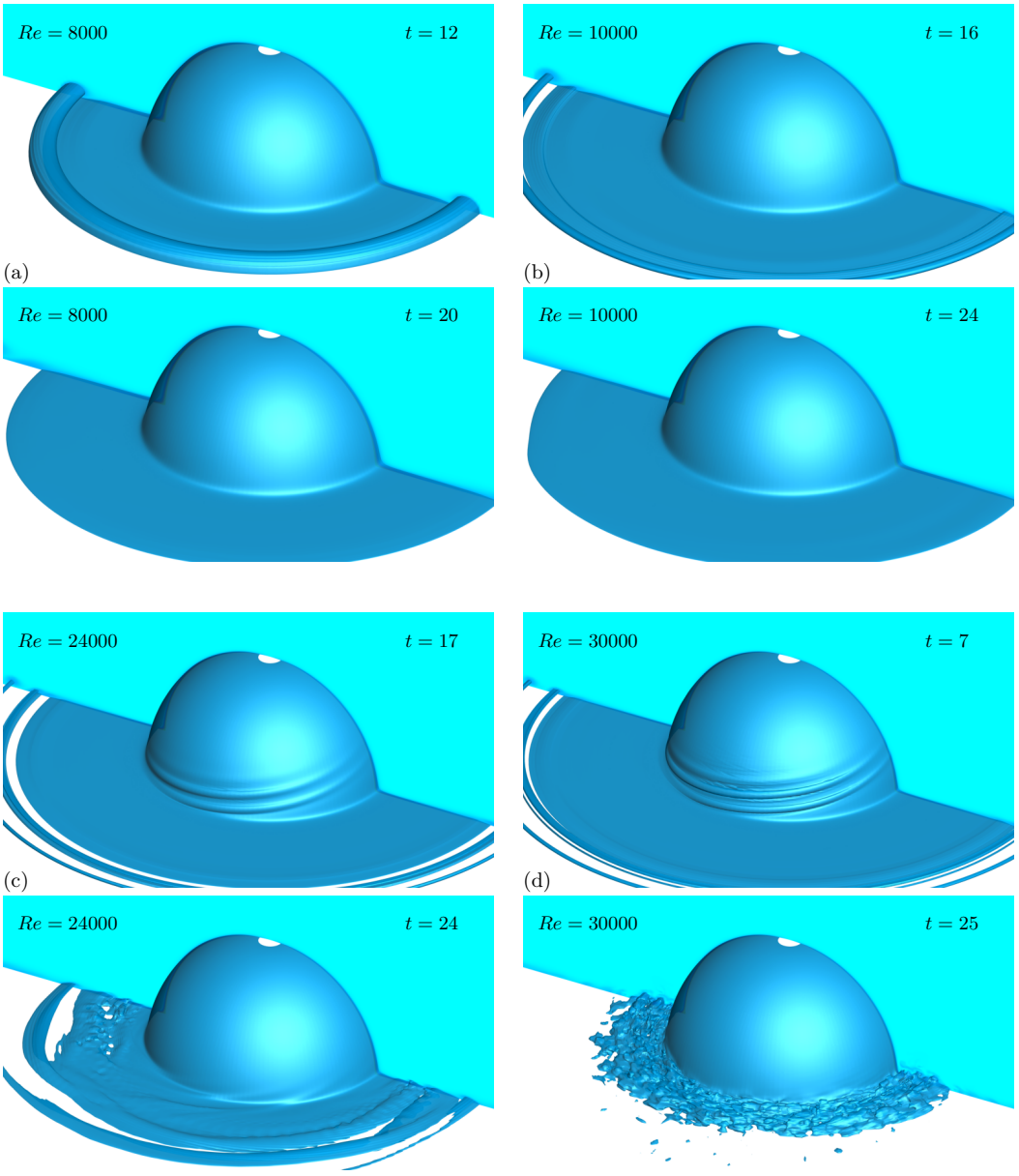

FIG. 2. Isosurfaces of the azimuthal velocity ($w = 0.1$), at various times, for flow Reynolds numbers (a) Re $= 8000$, (b) Re $= 10\,000$, (c) Re $= 24\,000$, and (d) Re $= 30\,000$.

"waterfall" plots in which we plot the azimuthal velocity versus radial distance (where $r = \cos\theta$) from the pole, using the notation that $r = 0$ is the pole and $r = 1$ is the equator, and versus time. This three-dimensional representation of the velocity field allows us to readily identify any development of the disturbance, introduced at a particular latitude, with time and observe how it propagates around the sphere (from its point of the introduction to the equator).

Our first set of results is presented in Fig. 1. Here we choose to present the azimuthal velocity at a (nondimensional) radial distance 0.02 units from the sphere's surface. This location is chosen as it lies within the boundary layer and provides a clear image of the development, and propagation,

TABLE I. Classification of the flow state for a variety of Reynolds numbers and for different latitudes for the introduction of the disturbance. A blank space indicates that no computation was performed in that particular regime.

Re	60°	70°	80°
8000	no instability	no instability	no instability
10000	transient	transient	no instability
11000	transient	transient	no instability
12000	transitional	transient	no instability
15000		transitional	
20000		transitional	
21000		transitional	
22000		transitional	
23000		transitional	
24000		transitional	
25000		transitional	
30000		turbulent	
40000		turbulent	

of the disturbance. Four different Reynolds numbers are shown. In each of the plots presented in Fig. 1, we have denoted a feature by the label A. This feature, which occurs at different times for different Reynolds numbers, is simply the last moments of the development of the radial jet and the subsequent ejection of the toroidal starting vortex (see [14,16] for a description of this early stage of the flow's development). This feature is of no further interest, in the context of the development of three-dimensional instability.

Turning now to the question of the development of three-dimensional instabilities, Fig. 1(a) shows a waterfall plot of azimuthal velocity at various latitudes, from $\theta = 70^\circ$ to $\theta = 0$, for a Reynolds number $\mathrm{Re} = 8\times10^3$. There is no evidence of an instability in this plot. For a slightly higher Reynolds number $\mathrm{Re} = 1\times10^4$, we see, in Fig. 1(b), the appearance of a disturbance (see label B), which grows with time while propagating towards the equator and then decays. Although the disturbance growth is evident in this plot, it is transient and any remnant of the instability is very quickly advected towards the equator, leaving no evidence of a disturbance in the boundary layer. This disturbance growth is more readily seen in Fig. 1(c), where we present results for a Reynolds number $\mathrm{Re} = 2.4\times10^4$. Although there is significant growth in the disturbance, the resulting spiral vortex is advected, through the boundary layer, down towards the equator. Figure 1(d), for a Reynolds number $\mathrm{Re} = 3\times10^4$, further demonstrates the now very significant growth, but also clearly shows that the disturbance is advected down to the equator and out into the radial jet. Thus, even at Reynolds numbers well above the threshold predicted for spiral vortex instabilities, the boundary layer on the sphere remains laminar or, more precisely, undisturbed over most of the sphere [the dashed line in Figs. 1(c) and 1(d) indicates the equator]. The plot presented in Fig. 1(d) also shows evidence of a secondary instability developing at a time of around $t = 15$ (see label C).

Although the pseudo-three-dimensional plots in Fig. 1 do provide some insight into the development and growth of an instability in the boundary layer, additional insight can be found from isosurfaces of the azimuthal velocity, presented in Fig. 2. The $w = 0.1$ isosurfaces are shown, taking in the whole flow domain on the sphere, at two different times for each image set (selected to demonstrate the main flow features). The isosurface for $\mathrm{Re} = 8000$, presented in Fig. 2(a), shows the developing radial jet (headed by the starting toroidal vortex) at time $t = 12$, which propagates away from the sphere leaving a laminar, unperturbed flow in the sphere's boundary layer. At a slightly higher Reynolds number, $\mathrm{Re} = 10\,000$ in Fig. 2(b), we see no clear evidence of the transient spiral vortex that was seen in Fig. 2(b), with the flow now appearing largely like that for the the case when $\mathrm{Re} = 8000$. Moving to higher Reynolds number $\mathrm{Re} = 24\,000$, shown in Fig. 2(c), the spiral

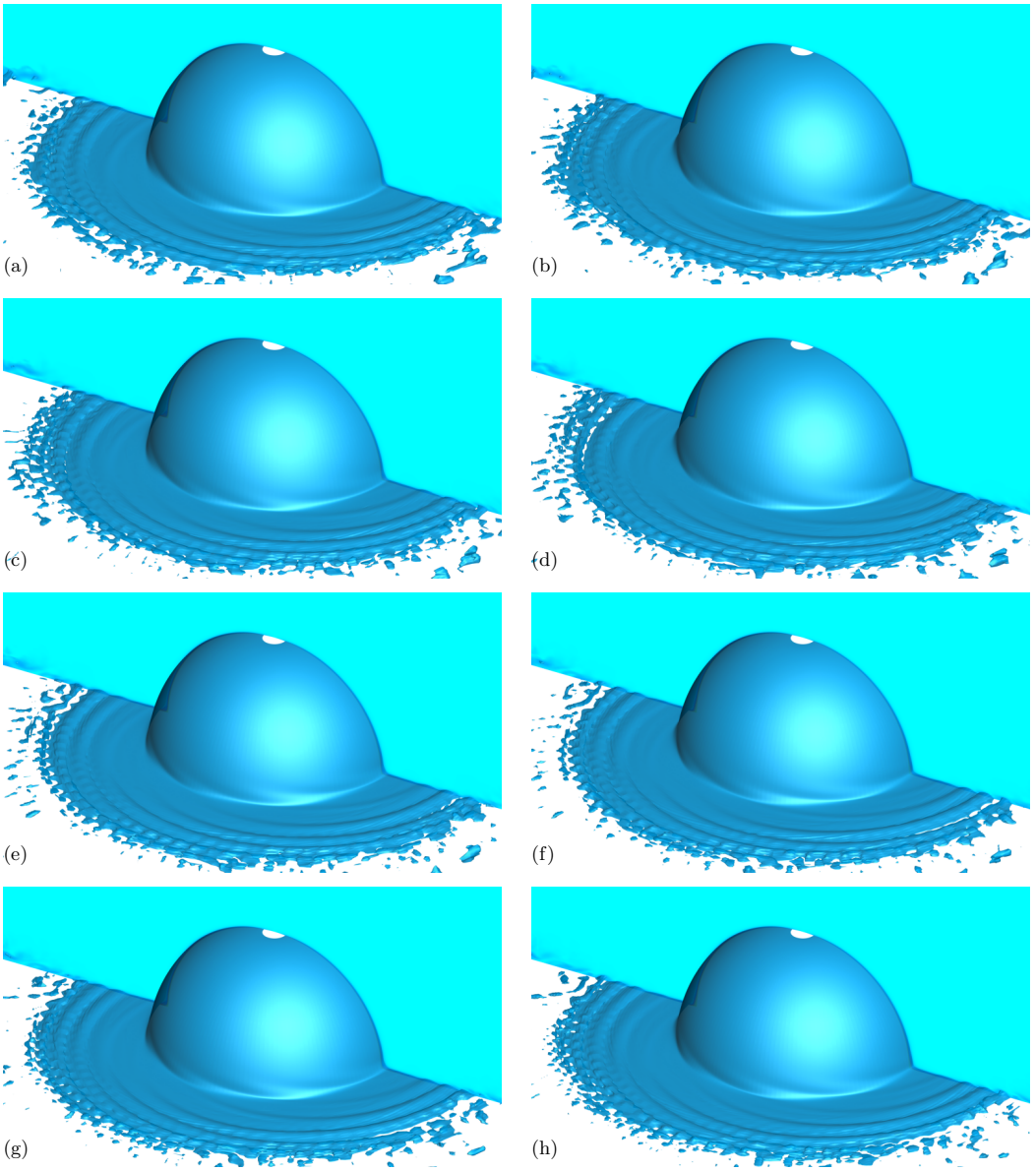

FIG. 3. Isosurfaces of the azimuthal velocity ($w = 0.1$) for a flow Reynolds number of Re = 25 000 at times $t = 40, 40.5, \ldots, 43.5$.

vortex, whose signature is first seen at time $t = 17$ in Fig. 2(c), can clearly be seen at a longitude of $\theta \approx 20^\circ$. This is advected towards the equator and into the radial jet, where its signature "spiral-arm" structure can be seen. At an even higher Reynolds number Re = 30 000, shown by Fig. 2(d), the spiral vortices are still clear, at time $t = 7$, but now show evidence of a secondary instability; we will return to a discussion of this flow feature in due course. At later times, the Re = 30 000 flow is seen to be laminar across a large proportion of the sphere's surface, except for the region near the equator where the radial jet has become turbulent. The full development of the flow, for this series of Reynolds numbers, can be found in the Supplemental Material [25].

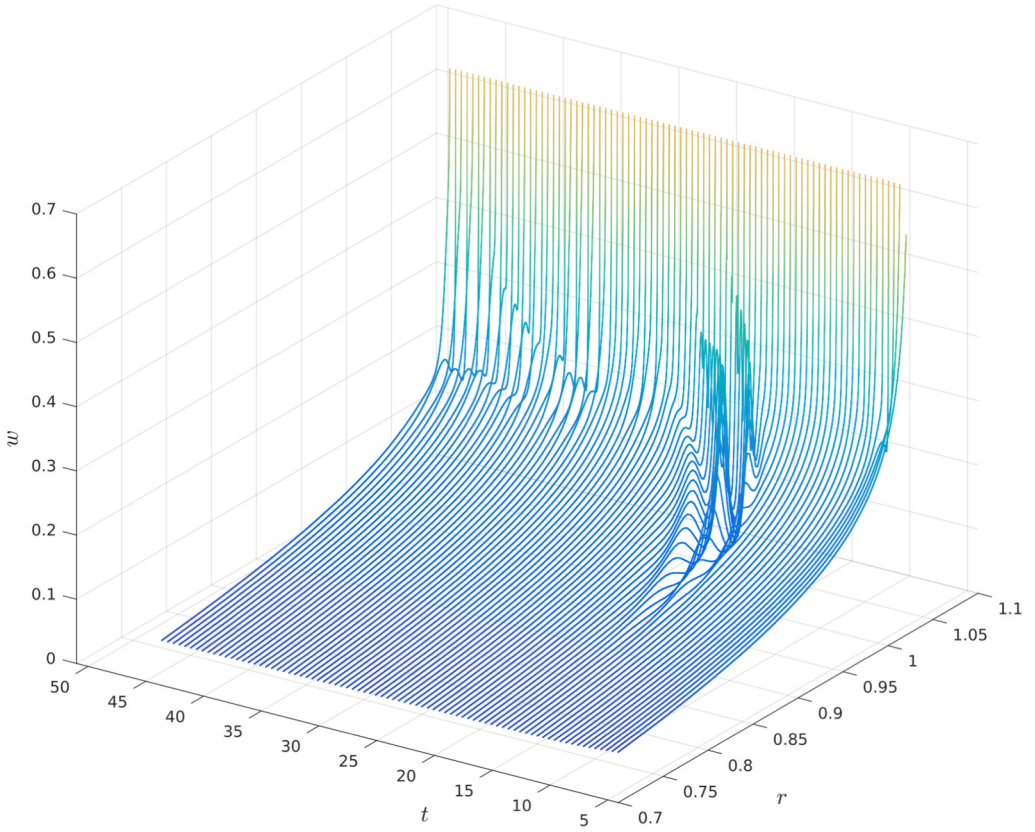

FIG. 4. The temporal evolution of the azimuthal velocity at 0.02 radii from the sphere's surface for a flow Reynolds number Re = 25 000, including the self-sustaining source of the spiral vortices in the radial jet.

All of the aforementioned results were obtained for a disturbance introduced at an angle $\theta = 70^\circ$ from the equator. The effect of changing the latitudinal location at which the disturbance is introduced is summarized in Table I. For each set of computational results, we classify the flow as *transient*, *transitional,* or *turbulent*. In the context of our results, a *transient* flow is one in which we see growth of the disturbance, which then decays, in the waterfall plots presented in Fig. 1; the amplitude of this disturbance is too small to observe in the isosurfaces presented in Fig. 2. *Transitional* indicates that spiral vortices (of varying strengths and amplitudes) are visible in both the waterfall plots and the isosurface image, but are advected down through the boundary layer and out into the jet. Finally, we use the label *turbulent* to describe those cases where the spiral vortices are still advected into the radial jet, but in which the flow within the jet becomes turbulent (and, perhaps, still showing some evidence of the three-dimensional spiral vortex signature).

Consider then the summary presented in Table I. When the disturbance is introduced at an angle $\theta = 80^\circ$ from the equator, no evidence of instability is found for Reynolds number up to, and beyond, the critical Reynolds number derived from linear stability theories. At a lower latitudinal angle, $\theta = 70^\circ$, the disturbance has varying impact upon the global flow. No evidence of instability is seen at Re = 8000; the flow shows only transient growth behavior for Reynolds numbers up to Re = 12 000. At Re = 15 000, the flow can best be described as transitional, a state that persists up to around Re = 25 000. For Reynolds numbers above this value, the flow is best described as turbulent, but still with the majority of the boundary layer on the sphere remaining laminar. Introducing the disturbance at a lower latitudinal angle, for example $\theta = 60^\circ$, serves to destabilize

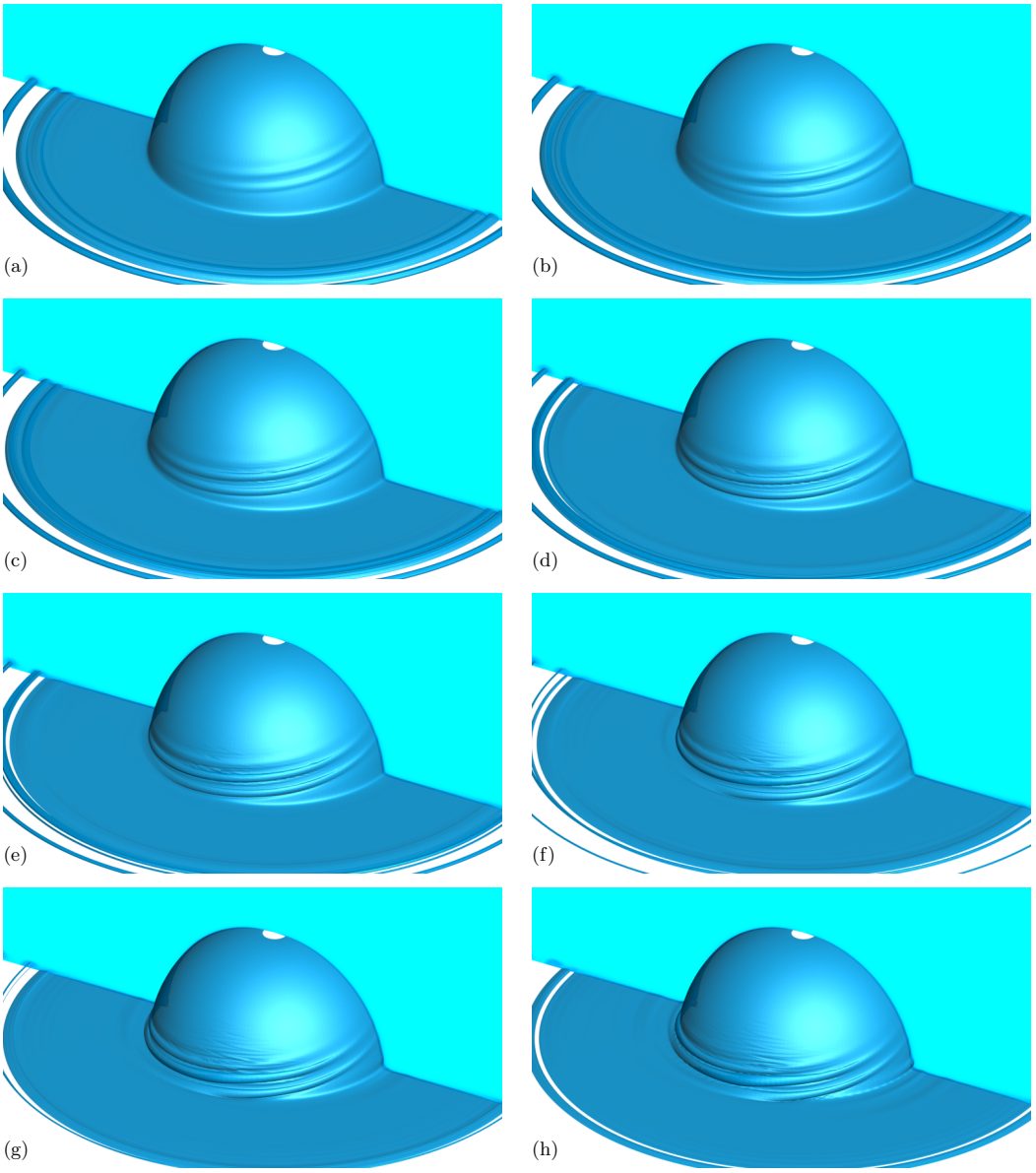

FIG. 5. Isosurfaces of the azimuthal velocity ($w = 0.1$) for a flow Reynolds number of Re $= 30\,000$ at times $t = 15, 15.5, \ldots, 18.5$.

the flow, with the flow moving into the transitional regime at a lower Reynolds number than for the $\theta = 70^\circ$ case.

The flow behavior at higher Reynolds numbers throws up a number of interesting phenomena, not described previously. Consider first the Re $= 25\,000$ case; when the disturbance is introduced at $\theta = 70^\circ$, we would classify this flow as transitional. The images presented in Fig. 3 show this transitional behavior in some detail. From these images, we can see the impact of the spiral vortices upon the radial jet. Although the boundary layer away from the equator is laminar, as we approach the equator a regular series of spiral vortices is generated and advected into the radial jet, giving the

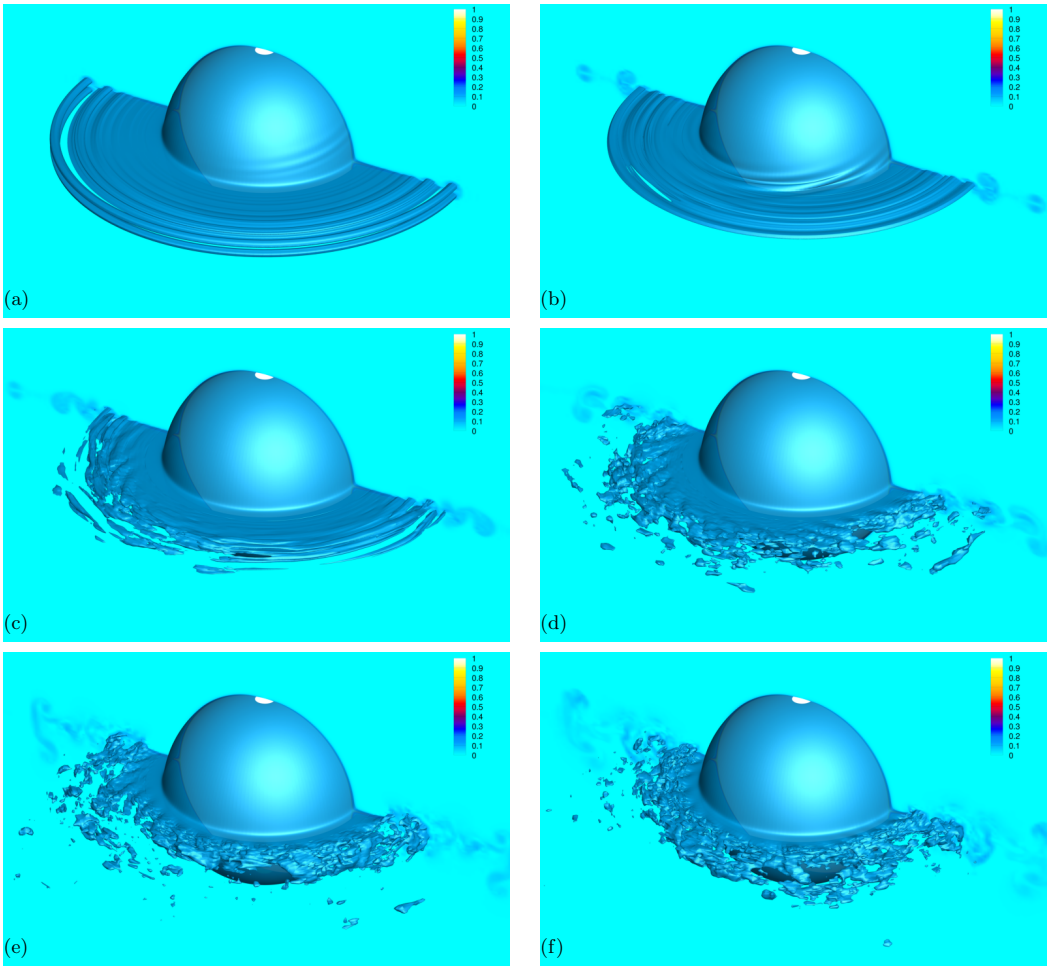

FIG. 6. Isosurfaces of the azimuthal velocity ($w = 0.1$) for a flow Reynolds number of Re $= 20\,000$ from a full half-sphere calculation. Shown are isosurfaces at times $t = 14, 19, \ldots, 39$. The full development of the flow can be seen in the accompanying video in the Supplemental Material [25].

flow a distinctive spiral-arm structure; this ultimately breaks up as the fluid in the jet is swept away from the sphere. These spiral vortices are self-sustaining, at this Reynolds number, as can be seen in the waterfall plot presented in Fig. 4. The development of the disturbance, at early times, followed by its decay is clearly seen. At later times, around time $t = 30$, a self-sustaining process of vortex generation near the equator occurs. This is more dramatically seen in the accompanying video in the Supplemental Material [25].

At a Reynolds number of Re $= 30\,000$, the flow ultimately becomes turbulent within the radial jet, but still remains laminar across most of the sphere. However, in its transition to this turbulent state, the flow exhibits the development of a secondary instability, emanating from the spiral vortex instability. This secondary instability can be seen in Fig. 5, which presents isosurfaces of the azimuthal velocity at various times; we observe the development of the spiral vortex in Figs. 5(a) and 5(b), the appearance of a secondary instability in Figs. 5(c)–5(e), leading to a patch of small-amplitude vortices, aligned in a direction opposite to that of the primary vortex in Figs. 5(f)–5(h). These secondary vortices closely resemble the "ringlike vortices" seen in the experiments of Kohama and Kobayashi [12] (see their Fig. 4). The full flow development, including

the ultimate transition to turbulence in the jet, can readily be seen in the accompanying video in the Supplemental Material [25].

We close this section with an observation concerning the fate of the "breakdown position" of the jet, defined by [13] as the radial distance from the sphere (at the equator) at which the jet becomes unstable. Hada and Ito's [13] experiments clearly show that this distance decreases with increasing Reynolds number, a fact confirmed by the computational work of Calabretto *et al.* [14]. Hada and Ito conjecture, based upon extrapolation of their experimental data, that this distance approaches unity (that is, the jet no longer exists) at a Reynolds number of around 33 000. We find no evidence of this critical shortening of the jet.

Before concluding this section, we revisit our earlier assumption that the flow over the sphere can be treated as symmetric with respect to the equatorial plane, an assumption that hinges upon the fact that the flow within the radial jet does not impact the flow within the sphere's boundary layer, as was so clearly demonstrated by Calabretto *et al.* [14]. We used this fact to support our approach of applying symmetry conditions on the flow at the equatorial plane, a condition which considerably reduces the computational burden of our calculations. Removing this symmetry condition allows the absolute instability in the radial jet, first described by [14], to develop in a natural manner. This absolute instability does not, however, impact upon the flow within the boundary layer, as can be seen in the series of images presented in Fig. 6. Here we have removed all symmetry conditions, solving for the full flow around the sphere, with no imposed symmetry along the equator. We can clearly see the various developmental stages described earlier: the developing spiral vortex [Fig. 6(a)] and subsequent secondary instability convected into the jet [Fig. 6(b)] leaving the sphere's boundary layer largely undisturbed [Fig. 6(c)]. Figure 6(d) shows the signature of the spiral vortex in the radial jet, and a shortening of the radial jet [Fig. 6(e)] prior to becoming fully turbulent [Fig. 6(f)] but still maintaining a region of laminar symmetric flow in the vicinity of the equator. The full development of the flow can be seen in the accompanying video in the Supplemental Material [25].

IV. CONCLUSION

We have presented a series of computations that explores the problem of transition to turbulence within the boundary layer induced by a rotating sphere. We have focused upon the question of how, where, and when the flow undergoes transition, aiming to understand the development of the spiral vortices that have been observed in earlier experiments. A key focus of our work has been understanding the disparity between two main bodies of experimental work, one of which demonstrates an instability in the form of spiral vortices at a Reynolds number of around 11 000, and the other body of experimental work showing no evidence of instabilities until much higher Reynolds numbers. Our computational results demonstrate that a disturbance introduced into the flow propagates away from the position at which it is introduced and is advected down through the sphere's boundary layer and out into the radial jet. After the passage of the disturbance, the flow over the large majority of the sphere remains laminar, in line with the experimental observations of [11] and [16].

For moderately high Reynolds numbers, the flow develops a self-sustained process of the generation of spiral vortices near the equatorial plane of the sphere, which are shed into and impact upon the structure of the radial jet. At even higher Reynolds numbers, the flow within the radial jet becomes fully turbulent (at suitably large post-spin-up times). This transition to turbulence is preceded by the development of secondary instabilities on the spiral vortices, similar in structure to the ringlike vortices observed in the experiments of [12]. Our results indicate that this secondary instability induces a tertiary instability, a patch of small-amplitude vortices, aligned in a direction opposite to that of the primary spiral vortex. This flow feature has some of the hallmarks of transient turbulent spots seen in wall boundary layers, and could be related to the observation by Ref. [11] that "direct visual observations ... showed that before transition actually occurred small turbulent spots originated in the flow" p. 891 and that these turbulent spots "broke up the laminar flow locally" p. 891.

In conclusion, we have shown that the boundary-layer flow generated by a rotating sphere is convectively unstable, and that any instability within the boundary layer is advected towards the equator and out into the radial jet. At suitably high Reynolds number, this jet breaks down, rendering flow in the equatorial jet fully turbulent.

We close by noting that a series of experiments, aimed at understanding roughness induced transition, is planned and we hope to be able to report on these in the near future.

ACKNOWLEDGMENT

The work of S.A.W.C. was supported by the Macquarie University New Staff Grant.

[1] L. Howarth, Note on the boundary layer on a rotating sphere, Philos. Mag. **42**, 1308 (1951).
[2] W. H. H. Banks, The boundary layer on a rotating sphere, Quart. J. Mech. Appl. Math. **18**, 443 (1965).
[3] W. H. H. Banks, The laminar boundary layer on a rotating sphere, Acta Mech. **24**, 273 (1976).
[4] W. H. H. Banks and M. B. Zaturska, The collision of unsteady laminar boundary layers, J. Eng. Math. **13**, 193 (1979).
[5] C. J. Simpson and K. Stewartson, A note on a boundary-layer collision on a rotating sphere, Z. angew. Math. Phys. **33**, 370 (1982).
[6] S. C. R. Dennis and P. W. Duck, Unsteady flow due to an impulsively started rotating sphere, Comp. Fluids **16**, 291 (1988).
[7] L. L. van Dommelen, On the Lagrangian description of unsteady boundary-layer separation. Part 2. The spinning sphere, J. Fluid Mech. **210**, 627 (1990).
[8] S. J. Cowley, L. L. Van Dommelen, and S. T. Lam, On the use of Lagrangian variables in descriptions of unsteady boundary-layer separation, Philos. Trans. R. Soc. London A **333**, 343 (1990).
[9] F. P. Bowden and R. G. Lord, The aerodynamic resistance to a sphere rotating at high speed, Proc. R. Soc. London A **271**, 143 (1963).
[10] F. P. Bowden and P. J. Harbour, The aerodynamic resistance to a sphere rotating at high Mach numbers in the rarefied transition regime, Proc. R. Soc. London A **293**, 156 (1966).
[11] F. Kreith, L. G. Roberts, J. A. Sullivan, and S. N. Sinha, Convection heat transfer and flow phenomena of rotating spheres, Int. J. Heat Mass Transfer **6**, 881 (1963).
[12] Y. Kohama and R. Kobayashi, Boundary-layer transition and the behavior of spiral vortices on rotating spheres, J. Fluid Mech. **137**, 153 (1983).
[13] T. Hada and A. Ito Visualization of breakdown process of vortex flows formed around a rotating sphere, Trans. Vis. Soc. Jpn. **23**, 231 (2003).
[14] S. A. W. Calabretto, B. Levy, J. P. Denier, and T. W. Mattner, The unsteady flow due to an impulsively rotated sphere, Proc. R. Soc. London A **471**, 20150299 (2015).
[15] S. A. W. Calabretto, J. P. Denier, and T. W. Mattner, The flow external to a rotating torus, Theor. Comput. Fluid Dyn. **30**, 295 (2016).
[16] S. A. W. Calabretto, J. P. Denier, and B. Levy, An experimental and computational study of the post-collisional flow induced by an impulsively rotated sphere (unpublished).
[17] D. Alciatore, Pool and billiards balls: Physical characteristics of pool balls, https://billiards.colostate.edu/ (unpublished).
[18] S. J. Garret and N. Peake, The stability and transition of the boundary layer on a rotating sphere, J. Fluid Mech. **456**, 199 (2002).
[19] A. Barrow, S. J. Garrett, and N. Peake, Global linear stability of the boundary-layer flow over a rotating sphere, Euro. J. Mech. B Fluids **49**, 301 (2015).
[20] A. Segalini and S. J. Garrett, On the non-parallel instability of the rotating-sphere boundary layer, J. Fluid Mech. **818**, 288 (2017).
[21] F. T. Smith and P. W. Duck, Separation of jets or thermal boundary layers from a wall, Quart. J. Mech. Appl. Math. **20**, 143 (1977).

[22] S. A. W. Calabretto, Instability and transition in unsteady rotating flows. Ph.D. thesis, The University of Auckland, 2015.

[23] J. P. Denier, P. Hall, and S. O. Seddougui, On the receptivity problem for Görtler vortices: Vortex motions induced by wall roughness, Philos. Trans. R. Soc. London A **335**, 51 (1991).

[24] H. M. Blackburn and S. J. Sherwin, Formulation of a Galerkin spectral element-Fourier method for three-dimensional incompressible flows in cylindrical geometries, J. Comput. Phys. **197**, 759 (2004).

[25] See Supplemental Material at http://link.aps.org/supplemental/10.1103/PhysRevFluids.4.073904 for videos of the $w = 0.1$ isosurface of the flow, for a variety of Reynolds numbers.